EARTHQUAKE ENGINEERING AND STRUCTURAL DYNAMICS, VOL. 26, 377–393 (1997)

ANALYSIS OF AMPLIFICATION CHARACTERISTICS OF GROUND MOTIONS IN THE HEAVILY DAMAGED BELT ZONE DURING THE 1995 HYOGO-KEN NANBU EARTHQUAKE

MASATO MOTOSAKA*

Earthquake Engineering Division, Disaster Control Research Center, Faculty of Engineering, Tohoku University, Aramaki-Aoba, Aoba-ku, Sendai 980-77, Japan

AND

MASAYUKI NAGANO†

Kobori Research Complex, Kajima Corporation, Tokyo, Japan

SUMMARY

To estimate the amplification characteristics of ground motions in the heavily damaged belt zone in Kobe City during the 1995 Hyogo-ken Nanbu earthquake, 3D wave propagation analyses of a 2D deep irregular underground structure model with a vertical discontinuity were performed at an early stage as a preliminary and qualitative study. The hyperelement method was applied to the analyses for incident plane waves expected from the wavefields due to the source mechanism. The observation records at Kobe University of the rock site were used as control motions. The ground motions on the engineering bedrock (assumed to be on the free surface of the Osaka group layers having a shear velocity of 500 m/s) and at ground surface were calculated. The effects of the deep irregular underground structure and shallow surface layers on the ground motion amplification are discussed. Although there are qualifications due to the uncertain characteristics of the input rock motion and shear wave velocities of the underground structure, the analytical results show that the ground motion in the heavily damaged belt zone were amplified due to the focusing effect of the deep irregular underground structure as well as the shallow surface layers, and that the calculated peak ground acceleration (PGA) distribution coincided closely with the distributions of structural damage.

KEY WORDS: Hyogo-ken Nanbu Earthquake; damaged belt zone; deep irregular underground structure; focusing effect; wave propagation analysis; hyperelement method

1. INTRODUCTION

A characteristic damage distribution occurred in Kobe City during the 1995 Hyogo-ken Nanbu earthquake, concentrated along the 1–2 km-wide heavily damaged belt zone[1] is shown in Figure 1. The highest death toll and most of the injured were concentrated in this zone, where the JMA seismic intensity was VII. The southernmost Rokko geological faults are also plotted as a broken line in Figure 1. It is noted that the heavily damaged belt zone is located south of the Rokko faults. Seismic observations recorded there very large velocity and acceleration amplitudes normal to the Rokko faults. The recorded peak ground acceleration (PGA) at Fukiai (FKI) in the belt zone exceeded 800 cm/s^2 and the PGA and the peak ground velocity (PGV) at Takatori (TKT) exceeded 600 cm/s^2 and 130 cm/s in two horizontal directions both in the belt zone, while the PGA observed at the Kobe University (KBU), in a rock site outside the belt zone, was about 300 cm/s^2 or less and the maximum velocity was 55 cm/s.[2,3] The locations of these and other observation sites are indicated in Figure 1.

* Associate Professor (formerly Kobori Research Complex, Kajima Corporation)
† Research Engineer

CCC 0098–8847/97/030377–17
© 1997 by John Wiley & Sons, Ltd.
Received 30 November 1995
Revised 17 September 1996

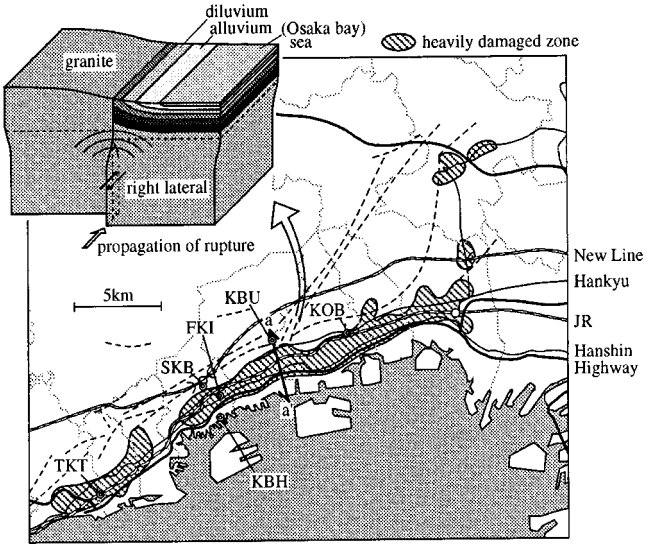

Figure 1. Heavily damaged zone in Kobe city during the 1995 Hyogo-ken Nanbu earthquake and schematic diagram of underground structure near Rokko fault zone. The JMA seismic intensity was VII in the hatched heavily damaged zone. The southernmost Rokko faults are plotted by a broken line. The a–a' line corresponds to the analysed section. The locations of the Hankyu line (HK), JR line (JR), and Hanshin line (HS) are indicated. Route 2 (R2) is located between JR and HS. Locations of major strong motion observation sites: Kobe University (KBU), Motoyama (KOB), Fukiai (FKI), Takatori (TKT), Shin Kobe (SKB), and the Kobe Harbor Office (KBH) are indicated

Why did the damage occur in this belt zone? Various explanations have been reported. Some reports suggest an unknown seismic fault beneath the belt zone.[4] Others propose that the ground motions were amplified by the interference of the horizontally propagating surface wave and the vertically propagating body wave in the shallow surface geology near the basin edge.[5] This interference of waves is sometimes called the '*Nagisa* phenomenon'. Is the shallow surface geology effect the only reason for the belt zone? At the very high amplitude level such that PGA exceeded 800 cm/s^2 and PGV 100 cm/s, the soil in general became a high damping material. Under these conditions the surface wave is unlikely to propagate because the wave is depressed by the high damping. Thus, the '*Nagisa* phenomenon' is unlikely to have occurred, while one-dimensional amplification due to vertically propagating body waves could be still expected. The authors focused their work on the deep irregular underground structure of the northwest edge of the Osaka Basin, and performed an analytical investigation[6] to verify their hypothesis that the damage in the belt zone was due to the amplification of ground motions due to focusing effects in the deep irregular underground structure as well as in the shallow surface layers. In this study, the phrase 'focusing effect' is used in its broadest sense, including amplification due not only to focusing of diffracted body waves at the irregular boundary and vertically propagated body waves, but also due to superposition of the basin-induced surface wave and the vertically propagating body waves in a deep irregular underground structure. The focusing effect has also been suggested by other authors, e.g. References 7 and 8, but they did not perform analytical investigations.

It is important in investigating the structural damage to various structures and the reconstruction of the damaged area to evaluate the features of the ground motions in the source area with strong geological variety normal to the fault by clarifying the phenomena through a simulation analysis. In this case, it is necessary to estimate the intensity of the ground motions not only on the ground surface but also at the upper surface of the Osaka group layers regarded as engineering bedrock (the shear wave velocity is 400–500 m/s).

This paper describes the wave propagation in two-dimensional (2D) irregular underground structure models across an orthogonal cross-section of the fault through Kobe University in Nada ward (refer to a–a′ line in Figure 1). The amplification characteristics of ground motion in the damaged zone from the Hankyu (HK) line through the JR (JR) line, Route 2 (R2), and Hanshin (HS) line to Route 43 (R43), are analytically

investigated. The distribution of structural damage near the a–a′ line is shown in Figure 17(b), while the analytically obtained PGA distribution is presented in Figure 17(a). Section 2 describes the underground structure model investigated. The analytical method is briefly described in Section 3. Section 4 addresses the ground motions at the surface of the Osaka group layers for incident plane waves expected from the wavefield due to the source mechanism. Two-dimensional in-plane analysis for the vertical incident S-wave is performed, as well as 3D (commonly called 2·5D) analysis for the obliquely incident SH-wave propagating along the fault. The latter incident wave field is assumed in Kobe in the direction in which the SH-wave was dominant in the source mechanism of the earthquake, namely, the strike slip of the vertical fault. These analyses use the observation record at Kobe University as control motion. Section 5 discusses the ground motions at the soil surface affected by amplification due to shallow surface layers indicating strong non-linearity. Section 6 compares the analytically estimated distribution of the PGAs to the distribution of structural damage, and the obtained peak values to those of the observation records. Section 7 presents some concluding remarks.

2. UNDERGROUND STRUCTURE AND ANALYTICAL MODEL

With regard to the deep underground structure around Kobe, corresponding to the northwest edge of the Osaka basin, there is a clear geological discontinuity along the fault between the mountain area and the sediment. Figure 2 shows the bedrock depth contours of the Osaka basin based on the geological survey and seismic refraction data.[9] In particular, boring data indicating 724 m at Ninomiya-cho, Chuo-ku, Kobe[10] have seen added in the figure. The gravity anomaly around the Osaka basin[11] also suggests a vertically discontinuous deep underground structure along the south foot of the Rokko mountains. This suggests that there are thick sediment layers to the south of the vertical discontinuity. From the top, an alluvium (Holocene) layer mainly consisting of sand with a shear wave velocity of roughly 200 m/s, diluvium (late Pleistocene) layers consisting of gravel with a shear wave velocity of about 300 m/s, Osaka Group layers, and weathered granite layers are stratified on the granite bedrock. The Osaka Group layers formed up to early Pleistocene consist mostly of sand and gravel. At the top of the Osaka Group layers, the shear wave velocity is about 400–500 m/s.

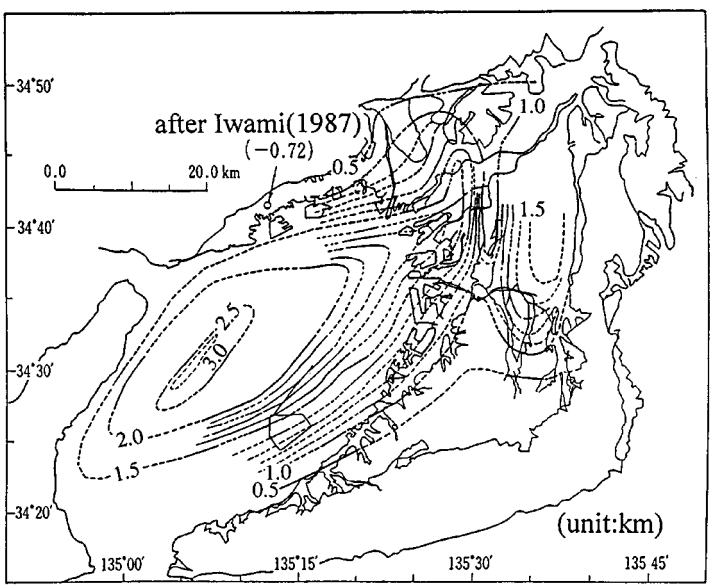

Figure 2. Contours of depth to bedrock in the Osaka basin based on refraction data and boring data.[9] Bedrock depth of − 0.72 km at Ninomiya-cho in Kobe, based on boring data,[10] is added

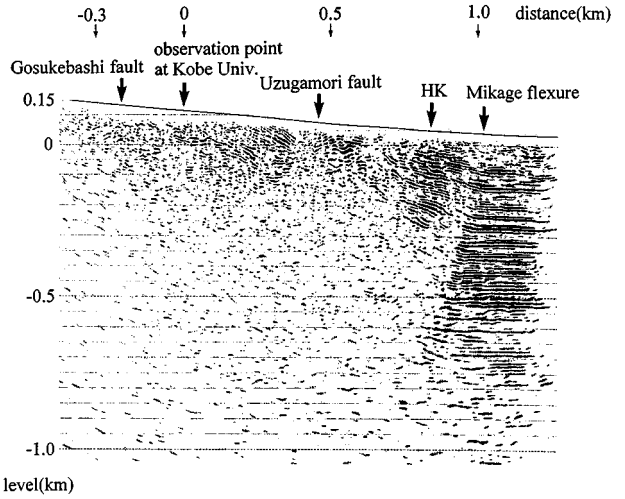

Figure 3. Seismic reflection profile along the Ishiyagawa line by the Committee of Earthquake Observation and Research in the Kansai Area[12]

In numerical modelling of a 2D section orthogonal to the Rokko fault, the following geological information is taken into account. The results of a reflection survey (refer to Figure 3), executed by the Committee of Earthquake Observation and Research in the Kansai Area (CEORKA), suggest that there is a major vertical discontinuity almost orthogonal to the Rokko fault beneath the Hankyu line along the Ishiyagawa measuring line, including the Kobe University site.[12] The velocity structure down to a depth of GL-70 m below the strong motion site at the Kobe University has also been investigated by CEORKA.[12]

The two 2D models shown in Figure 4 were used in this study. The shallow surface layers, having a total thickness varying from 10 to 100 m and indicating strong non-linearity during the earthquake, are excluded. The effects of these layers are evaluated later by one-dimensional non-linear analysis (equivalent linear analysis) as described in Section 5. The sediment below the Osaka group is modeled as a two-layer structure. Tables I–III list the soil properties of the layered model used for the rock site, for the transition zone between the rock and sediment site, and for the sediment site. The assumed velocity structure for the rock site is determined from the geological structure by CEORKA[12] and Iwata *et al.*[13] The velocity structure of the sediment site is also based on Iwata *et al.* (1995), being determined from the delay in arrival time due to the sediment layers for the SP-converted waves of an aftershock. It is noted that the Q-value of each layer is assumed to be Vs (m/s) /15. The dispersion curves of the fundamental modes of the surface waves for these velocity structures are shown in Figures 5(a) and 5(b) for the rock site and sediment site, respectively, for consideration of wave propagation of the secondary generated surface waves at the rock-sediment boundary.

The two analytical models in Figure 4, MODEL 1 and MODEL 2, are used in the wave propagation analyses to investigate the sensitivity of the vertical discontinuous part in the underground structure. MODEL 1, with 3-hyperelements,[14] has two vertical discontinuities. The transition zone is defined between the two vertical boundaries. MODEL 2 is a simplified version having only two hyperelements.

3. ANALYTICAL METHOD

The hyperelement method is applied to the wave propagation analysis of the 2D models described above. This method was originally proposed by Kausel and Roesset[15] for the 2D plane strain and axisymmetric cases. The authors have extended it to the 3D response problem of the 2D structure for incident plane waves with arbitrary azimuth and incident angles.[14] In this method, an analysed structure is divided into several regions with horizontal layers. Each region is modelled using a hyperelement. The nodes of the hyperelement are placed at the interfaces of the thin-layer elements on both sides of a region. The displacement at an

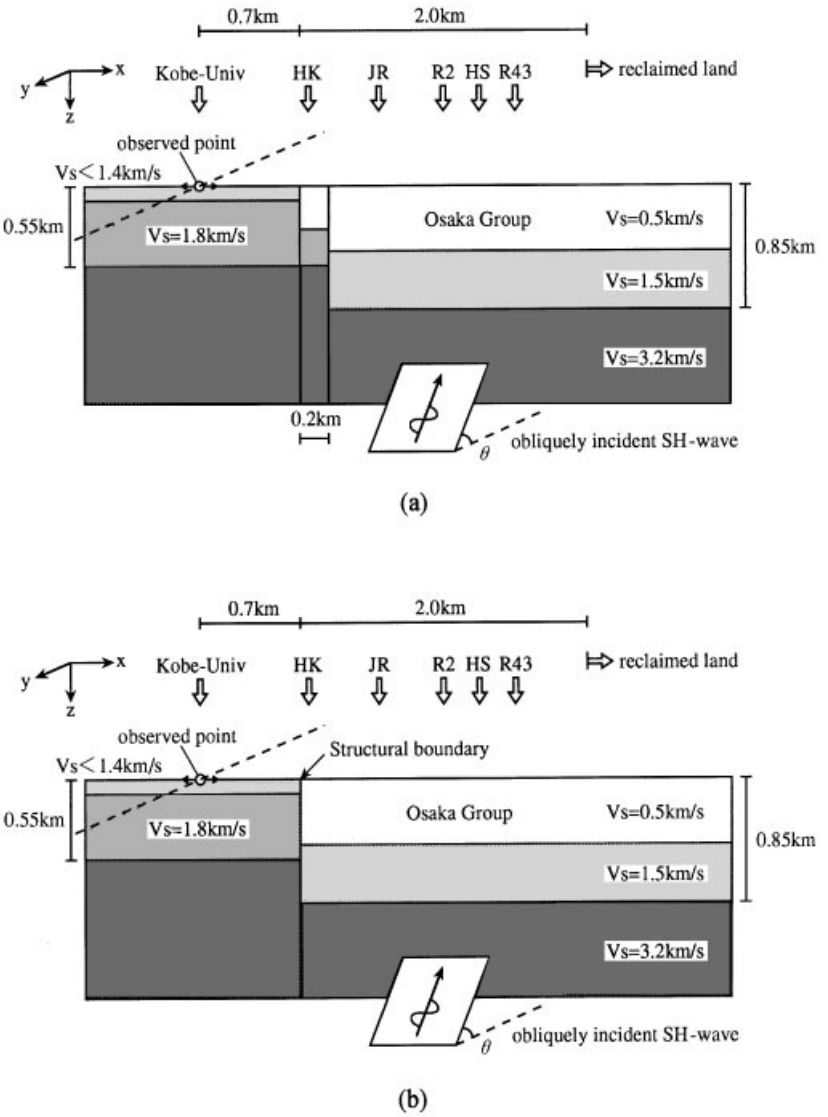

Figure 4. Two-dimensional models of underground structure orthogonal to the Rokko fault plane: (a) MODEL 1 and (b) MODEL 2. HK, JR, R2, HS and R43 indicate the Hankyu line, JR line, Route 2, Hanshin line and Route 43 (Harbor Expressway), respectively. The 3D wave propagation characteristics are investigated for the incident SH-wave propagating along the underground structure with a vertically incident angle of θ. The incident wave is expected from the wavefield from the source mechanism of nearly strike slip of the vertical fault

arbitrary internal point in the hyperelement is calculated using an interpolation function specified as the wave function, once nodal displacements are obtained. Each node has three degrees of freedom. The method enables 3D response analysis not only for incident body and surface waves, but also for a source moving at a constant velocity.

The frequency range of the analyses is from 0 to 10 Hz. For the two models (MODELs 1 and 2), 2D in-plane response analyses are first performed. For MODEL 2, the 3D response analysis is performed for an obliquely incident SH-wave propagating along the 2D irregular structure. The vertical incident angle is assumed to be 45°, taking into account of the source's location. It is noted that the SH-wave is dominant in the location in Kobe City for the seismic waves from the source with the source mechanism of nearly strike slip of

Table I. Soil profile of rock site in MODELS 1 and 2

Layer no.	V_s (m/s)	V_P (m/s)	γ (t/m^3)	thickness (m)
1	850	2050	2·1	12·2
2	960	2250	2·1	7·45
3	1120	2850	2·1	12·5
4	1350	3100	2·2	67·85
5	1800	5500	2·4	450·0
6	3200	5700	2·5	∞

Table II. Soil profile of transition zone in MODEL 1

Layer no.	V_s (m/s)	V_P (m/s)	γ (t/m^3)	thickness (m)
1	500	2200	2·1	300·0
2	1800	5500	2·4	250·0
3	3200	5700	2·5	∞

Table III. Soil profile of sediment site in MODELS 1 and 2

Layer no.	V_s (m/s)	V_P (m/s)	γ (t/m^3)	thickness (m)
1	500	2200	2·1	450·0
2	1500	2800	2·2	400·0
3	3200	5700	2·5	∞

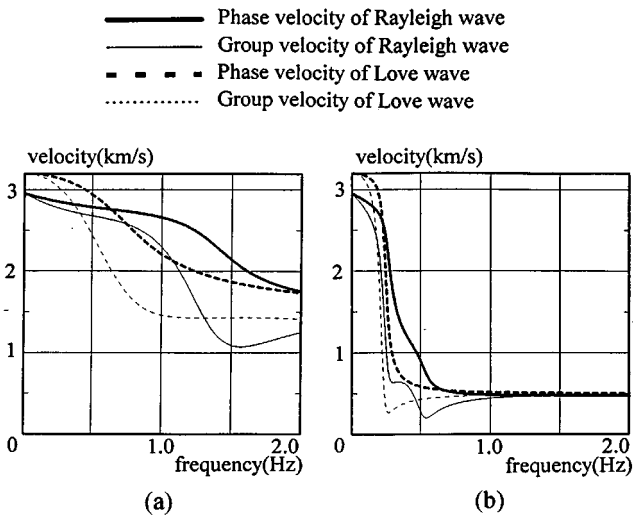

Figure 5. Dispersion curves of fundamental modes of Love and Rayleigh waves: (a) Rock site and (b) sediment site

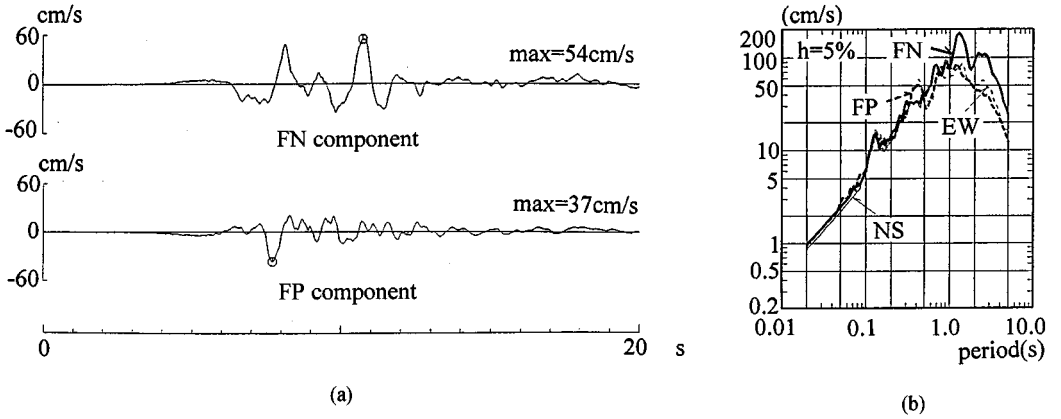

Figure 6. Rotated waveforms and corresponding pseudo-velocity response spectra: (a) Rotated velocity waveforms; (b) pseudo-velocity response spectra ($h = 5\%$). The thick lines are the spectra of rotated waveforms and the thin lines are those of original observed waves in the NS and EW directions

the vertical fault. The waveforms are calculated by the commonly used frequency response analysis using Fast Fourier Transform (FFT).

The velocity ground motions in the NS and EW directions observed at Kobe University by CEORKA[2] are rotated to components fault normal (FN, N160° E) and fault parallel (FP, N250° E), that is, 20° to the EW direction. The rotated waveforms and the corresponding pseudo-velocity response spectra are shown in Figure 6, where it is noted that the peak at around 2·5 s of the response spectrum in the original EW component disappears in the FP component. In the simulation analysis the velocity waveform in the FN component is used as a control motion at the location of Kobe University after eliminating the effects of the soft weathered granite layers with shear wave velocities of less than 850 m/s by 1D equivalent linear analysis. That is, the incident waveform is determined such that the calculated waveform becomes the control motion at Kobe University. It is noted that the x, y, and z directions defined in Figure 4 correspond to the FN, FP, and UD directions, respectively.

4. GROUND MOTION CHARACTERISTICS IN ENGINEERING BEDROCK

Firstly, the amplification characteristics in the sediments of the two models are compared for the 2D in-plane analysis for the vertically incident S-wave. The PGVs of the two models are compared in Figure 7. The PGVs of the soil site by the 1D analysis for the sediment are indicated by the thin broken line. This figure shows that the overall shapes of the PGV distributions for Models 1 and 2 are almost the same. The sensitivity of the amplification characteristics to the transition zone is small. The horizontal PGV increases with distance from the rock–sediment boundary. The peak values are largest in the range of 0·5–2·5 km from the boundary. The maximum amplification factor at the sediment to rock is about 2·5 in the two models, and it occurs at the 0·8 km point between JR and R2.

In the reclaimed land region, the PGV decreases as the points approach the sea side. It is recognized that the PGVs of the 2D analyses are about 75 per cent larger than those of the 1D analysis at around the 0·8 km point and 60 per cent larger at the 1·8 km point from the rock-sediment boundary. As can be seen from this figure, the vertical PGV induced by the irregular underground structure is large in the sediments near the rock and decreases with distance from the boundary. The ratios of vertical PGV and horizontal PGV are less than 0·5, except in the boundary region from 0 to 0·5 km.

To investigate the amplification in the 2D analyses, the calculated waveforms for MODEL 2 are shown in Figures 8(a), 8(b), and 8(c) for the total wavefield in the FN direction, the total wave field in the UD direction and the scattered wavefield in the FN direction, respectively. The scattered wavefield is defined as the

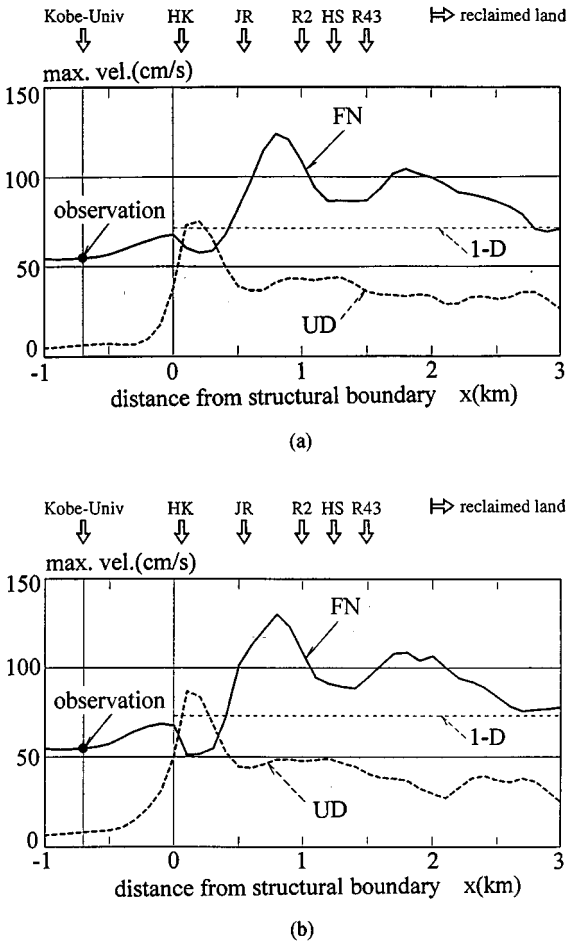

Figure 7. Distribution of PGVs at surface of Upper Osaka group (for MODELS 1 and 2 subjected to vertically incident S-wave). (a) MODEL 1 and (b) MODEL 2. The solid line indicates the distribution of PGVs in the FN direction. The broken line indicates those in the UD direction. The thin broken line indicates the PGV by the 1D analysis

subtraction of the incident wavefield (i.e. the wavefield obtained by 1D analysis using the velocity structure of the sediment site) from the total wavefield. The arrows in Figures 8(b) and 8(c) at the rock-sediment boundary correspond to wave propagation at the group velocity (0·24 km/s) of the fundamental mode of Rayleigh wave in the Airy phase. It is recognized that the amplitudes of the scattered waveforms in the FN direction do not decrease monotonically but fluctuate in space, and only the waves in the latter part of the waveforms propagate at a velocity of 0·24 km/s. This means that the scattered waveforms consist mainly of body waves due to refraction at the rock–sediment boundary and their transmitted and reflected waves at the layer boundaries of the sediment site, rather than of the basin-induced surface waves which contribute to the dispersive waveforms of the total wavefield. The amplification of ground motions between the JR line and R2 seems to be caused by superposition of the vertically propagating body waves and the scattered waves comprising various diffracted waves. The amplification of ground motion due to the superposition of the waves passing through different paths seems to produce a kind of focusing effect. Dispersive wave propagation can also be seen in the induced vertical motions. It is recognized that, except for those of the latter part of the waveforms, the waves propagate at a higher velocity than 0·24 km/s. The duration increases with distance from the vertical discontinuity. That is, the duration at the 3 km point from the rock–sediment boundary becomes 15 s, compared to 6 s at Kobe University.

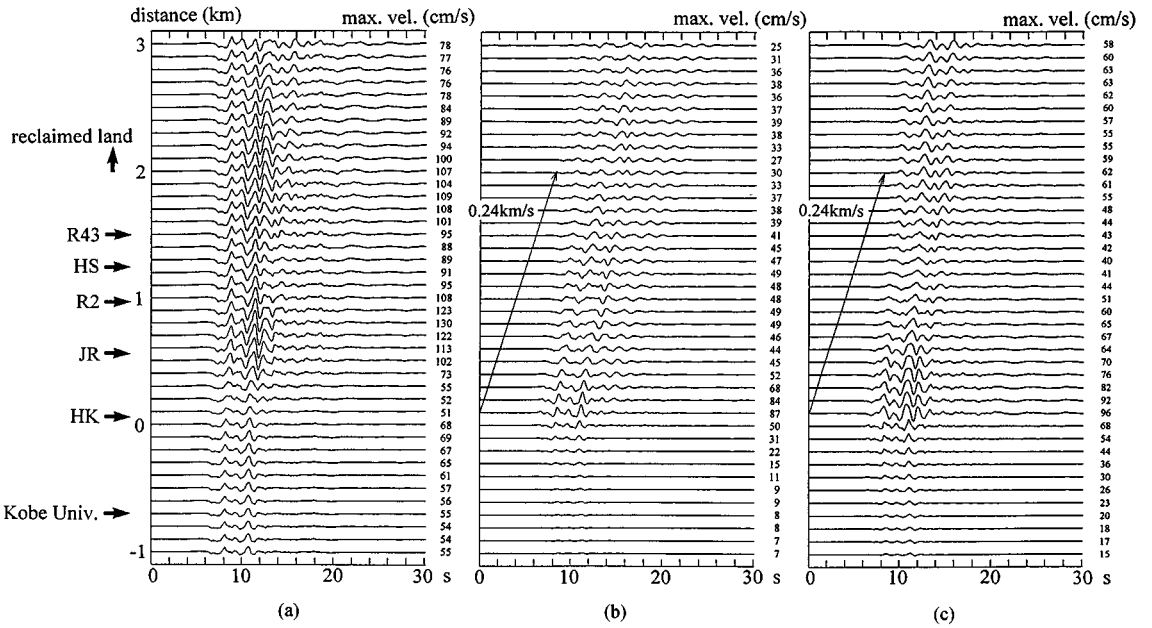

Figure 8. Calculated velocity waveforms at surface of MODEL 2 subjected to vertically incident S-wave: (a) FN direction, (b) UD direction, and (c) Scattered wave contents in the FN direction. The arrows in (b) and (c) at the rock–sediment boundary correspond to the wave propagation at the group velocity of the fundamental mode of Rayleigh wave in the Airy phase

Next, the 3D response characteristics due to an obliquely incident SH-wave are investigated using MODEL 2. The calculated velocities in the FN, FP, and UD directions are shown in Figures 9(a), 9(b) and 9(c). The PGV in the FN direction becomes 126 cm/s at the 1 km point from the rock–sediment boundary, compared to 55 cm/s at Kobe University. The waveforms in the FP direction are the induced horizontal motions at the rock–sediment boundary consisting mostly of anti-plane motions including Love waves. The arrow in Figure 9(b) corresponds to the wave propagation at the group velocity (0·27 km/s) of the fundamental mode of Love wave in the Airy phase. Wave propagation characteristics in the FN and UD directions are similar to those of the vertically incident case.

Figures 10(a) and 10(b) show the PGV and PGA distributions for MODEL 2 subjected to the obliquely incident SH-wave. The PGVs in the FN and FP directions are almost equal but slightly larger than those in the vertically incident case. The PGV in the FP direction is less than half than that in the FN direction. The shape of the PGA distribution is similar to that of the PGV distribution, indicating that the peak values become large at around the 0·8 km point from the rock–sediment boundary, where the PGAs become 800 cm/s^2 versus 300 cm/s^2 at the rock site at Kobe University.

In Figure 11, the velocity waveforms at various points on the sediment sites are compared to those of the 1D analysis. It is recognized that the interference due to the scattered waves caused by the rock–sediment boundary occurs at a later time with increasing distance from the boundary, as marked in this figure.

The acceleration response spectra at the same points are compared to those of the 1D analysis in Figure 12. The shapes of the spectra are almost equal and the spectral values are proportional to the PGAs at points P-1 and P-2. At points P-3 and P-4, far from the structural boundary, the spectral shapes and values are almost the same as those of the 1D analysis. The spectral values at P-2 are amplified in the wide period range shorter than 4 s.

It is confirmed from above-described investigation that the ground motions between JR and R2 are amplified by superposition of the vertically propagating body waves and the scattered waves including body and surface waves from the rock–sediment boundary, which can be interpreted as a focusing effect.

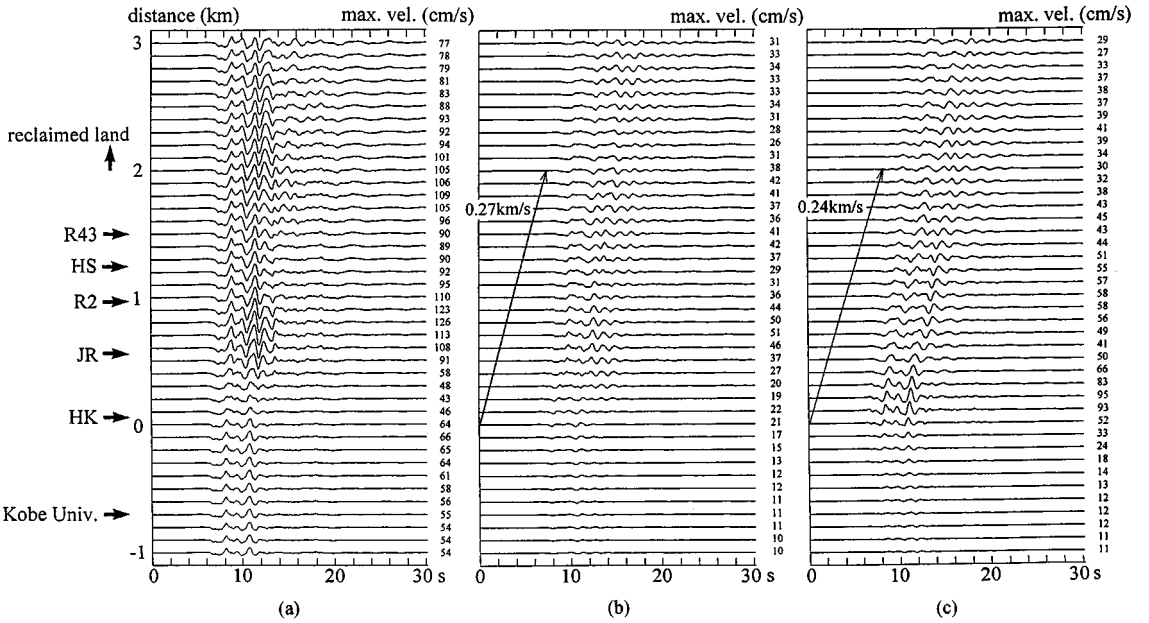

Figure 9. Calculated velocity waveforms at surface of MODEL 2 subjected to obliquely incident SH-wave. (a) FN direction, (b) FP direction, and (c) UD direction. The arrows in (b) and (c) at the rock–sediment boundary correspond to the wave propagation at group velocities of the fundamental modes of Love wave and Rayleigh wave in each Airy phase

5. SURFACE GROUND MOTION CHARACTERISTICS TAKING ACCOUNT OF SHALLOW SURFACE LAYERS

To estimate the non-linear soil amplification due to the shallow surface layers, a 1D non-linear wave propagation analysis is performed using waveforms calculated at equally spaced points (100 m) on the surface of MODEL 2 subjected to the obliquely incident SH-wave. A conventional equivalent linear analysis using computer-code SHAKE was performed, as a practical method of estimating the distributions of PGVs and PGAs, taking into account the relatively small effect of liquefaction in the heavily damaged region. Input motions were located on an outcrop of the Osaka Group. The diluvium and alluvium layers on the Osaka Group layers were taken into account in this analysis. Figure 13 shows the configuration of these shallow surface layers, which was determined based on the boring data.[16] The thickness of these layers increases toward the sea side.

The assumed small-strain shear wave velocities of the alluvium and diluvium layers are 200 and 300 m/s. Their corresponding densities are 1·6 and 1·8 t/m^3. The modulus reduction ($G/G_0 - \gamma$) and modulus damping ($h - \gamma$) curves of the two layers are shown in Figure 14. These curves are based on the average nonlinear soil characteristics reported by Imazu and Fukutake.[17]

Figures 15(a) and 15(b) show the distributions of PGV and PGA taking into account the amplification due to shallow surface layers indicated by the thick solid lines. To compare the obtained results with those of the 1D analysis for all sediment layers on the granite bedrock without considering the irregularity of the deep underground structure, the latter are indicated by thick broken lines. In this figure, the distributions of the peak values on the free surface of the Osaka group are also shown by thin lines for comparison. 'SUOG' in this figure stands for the Surface of the Upper Osaka Group. It is found from this figure that the PGVs and accelerations at the ground surface become large between JR and R2, where the ratios of the structural damage are very high, as shown later in Section 6. The PGVs and PGAs in the damaged zone are amplified up to 3–4 times those at the rock site. The PGA from 0·5–1·5 km is much larger (50%) than that of the whole

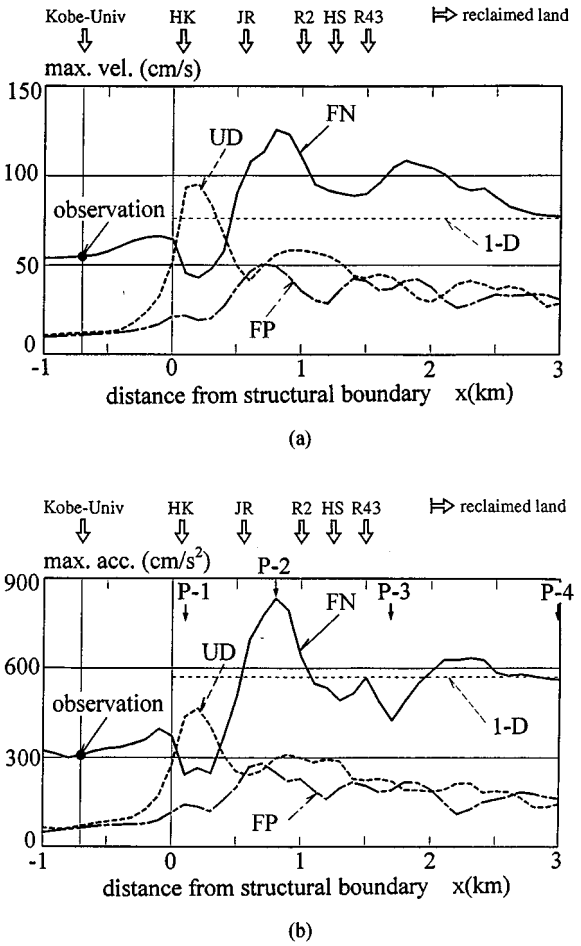

Figure 10. Distribution of peak values at surface of MODEL 2 subjected to obliquely incident SH-wave ($\theta = 45°$) : (a) PGV and (b) PGA. The solid line indicates the distribution of PGVs in the FN direction, the chain line in the FP direction, and the thick broken line in the UD direction. The thin broken line indicates the PGV by the 1D analysis

1D analysis. It is suggested that the amplification of ground motions between JR and R2 seems to be caused by the focusing effects of the deep irregular underground structures. However, as the points approach the sea side, the PGAs are almost the same as those of the 1D analysis. It is recognized that the PGVs at the ground surface are large over a wider area than the PGAs. This means that the longer period content contributing to the PGVs is amplified due to the surface layers' increasing depths toward the sea side, compared to the shorter period contents contributing to the PGAs.

Figure 16 shows the acceleration response spectra for 4 major points, P-5 to P-8, of locations indicated in Figure 15. It is found that the spectral amplification at the 0·8 km point from the rock–sediment boundary is significant at periods 0·6–0·7 s. With increasing distance from the rock site, spectral values of a longer period range are amplified.

It is noted that the maximum shear strain calculated in the shallow surface layers is about 1·2 per cent at the 0·9 km point from the rock–sediment boundary. This strain is large, but may not be beyond the applicable level of the equivalent linear analysis for estimating the PGAs and PGVs. Although the effects of liquefaction may not be disregarded, especially south of the R43, it may not be unreasonable to estimate PGA or PGV with SHAKE in the area of calculation, assuming that the effect of cyclic mobility on PGA is small. SHAKE was used in estimating the 1D amplification of the surface layer in this study, first because the

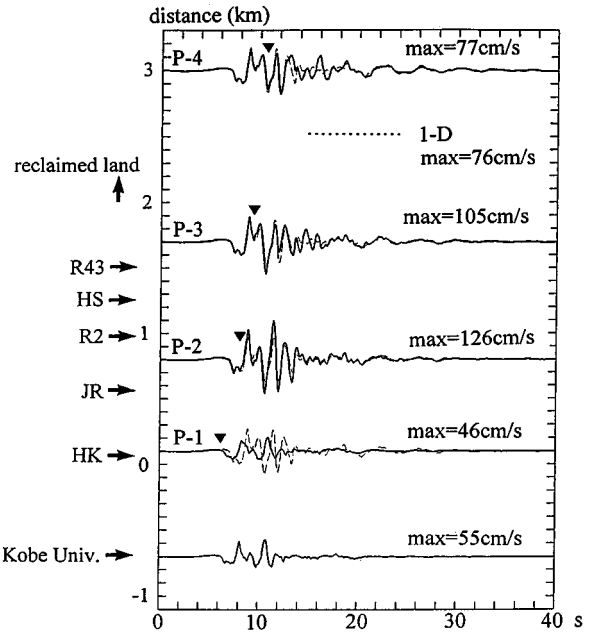

Figure 11. Comparison of calculated velocity waveforms of MODEL 2 and the 1D soil model subjected to obliquely incident SH-waves ($\theta = 45°$). The solid lines indicate the waveforms by MODEL 2 and the broken lines indicate those by the 1D soil model. The interference seems to occur roughly from the marked time

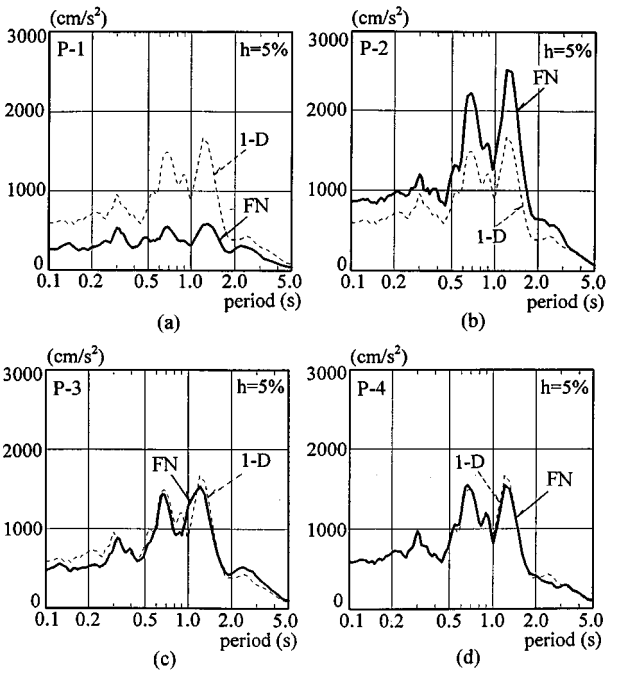

Figure 12. Acceleration response spectra at surface of MODEL 2 subjected to obliquely incident SH-wave ($\theta = 45°$). (a) P-1, (b) P-2, (c) P-3, and (d) P-4

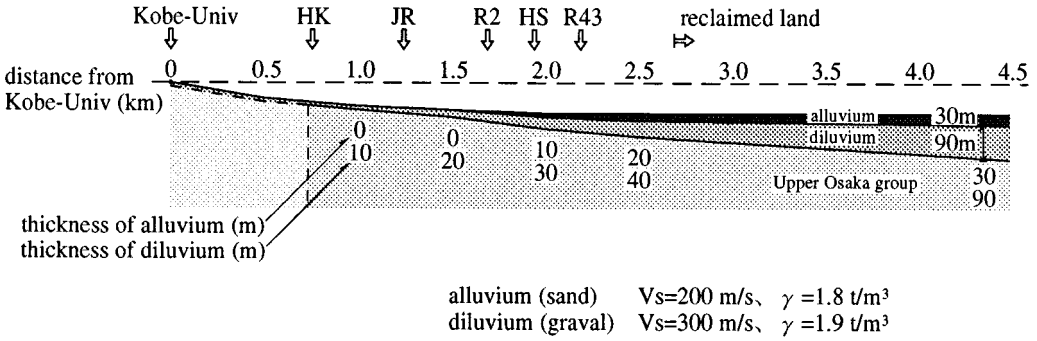

Figure 13. Configuration of shallow surface layers. The 1D equivalent linear analysis is performed at equally spaced points with 100 m separation using the calculated waveforms at the surface of MODEL 2 at the corresponding locations

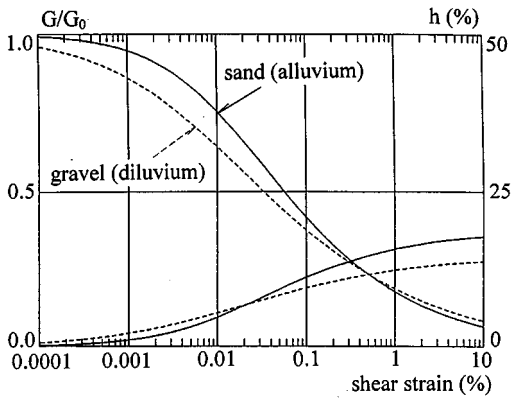

Figure 14. Non-linear characteristics of soils, $G/G_0 - \gamma$, $h - \gamma$. G/G_0, h and γ are shear modulus ratio, damping coefficient and shear strain, respectively

authors focused mainly on the 'heavily damaged belt zone', where the effect of liquefaction is considered to have seen relatively small, second because the soil parameters including liquefaction factor needed for more exact calculations are not yet clear, and third because SHAKE is a practical, useful and generally accepted tool for estimating 1D amplification factors.

6. DISCUSSION

6.1. Comparison of the distributions of structural damage and PGAs

Figure 17 compares the calculated distribution of PGAs and observed structural damage ratio (for wooden structures and reinforced concrete structures) near the analysed section in Nada ward. Damage ratio is defined as the ratio of the number of heavily damaged and collapsed structures to the total number of structures of that type. Figure 17(b) indicates both the data by Ono *et al.*[18] and by Akamatsu *et al.*[7] It is noted that the investigated line by Akamatsu *et al.* is a little different from that by Ono *et al.*, although both are NS lines near Kobe University. Comparing this figure with Figure 17(a), it is found that the shapes of the calculated PGA distributions coincide closely with the distribution of structural damage by Ono *et al.* It is recognized that the damage distribution by Akamatsu *et al.* differs slightly from that of Ono *et al.* near Kobe University, in that the damage ratios in the north part of Hankyu line is relatively high compared to those of

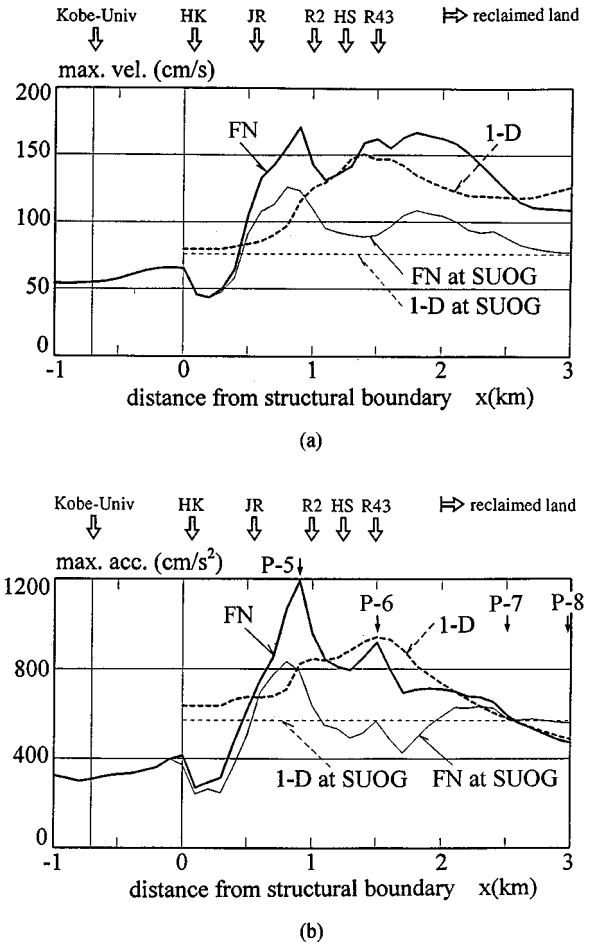

Figure 15. Distribution of peak values at ground surface (for MODEL 2 subjected to obliquely incident SH-wave) : (a) PGV and (b) PGA. SUOG stands for 'Surface of Upper Osaka group'

Ono *et al.* One of the main reasons may be the complex surface geology in the area of the investigated line by Akamatsu *et al.*, but not yet clarified. Chuo Kaihatsu Corporation[19] performed a systematic damage survey to obtain the damage distribution over a wide range of Kobe City, and the damage distribution referred from of Ono *et al.* comprises the results of a cross-section near the analysed section shown in Figure 1. In that sense, their result is rather reliable in indicating the damage ratio in Kobe City. It seems that the distribution of the line by Ono *et al.* represents better the average damage distribution in the neighbourhood area of Kobe University, compared to Akamatsu *et al.*

It is also recognized by comparing the calculated PGA distribution (Figure 17(a)) and the structural damage ratio by Ono *et al.* (Figure 17(b)) that the PGAs in the region where the damage ratios exceed 50 per cent are 800–1200 cm/s^2.

It is noted that the results discussed above are based on the analyses using the 2D model with preliminary assumed velocity structures for deep and shallow layers. The incident wave is assumed to be a plane wave which is estimated by a deconvolution analysis using the observation record at Kobe University. The sensitivity of the results to the characteristics of the input rock motion and shear wave velocities of subsurface materials including significant sources of uncertainty, should be further investigated to quantitatively discuss the results at the next stage.

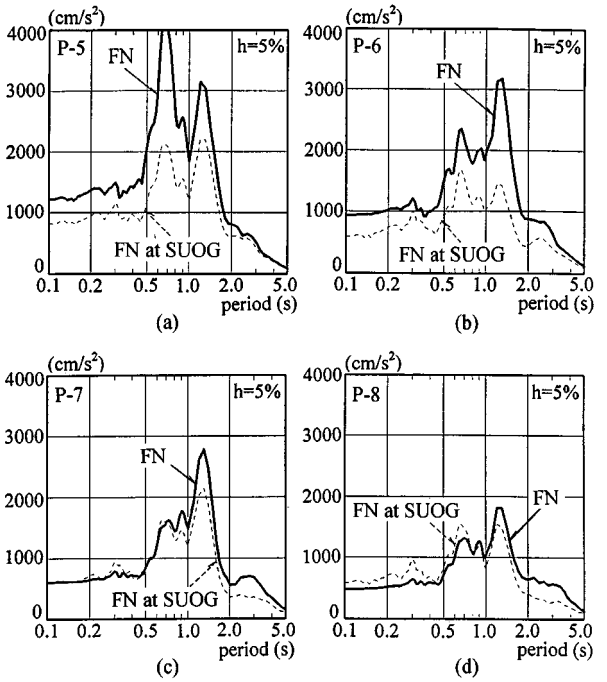

Figure 16. Acceleration response spectra at ground surface (for MODEL 2 subjected to obliquely incident SH-wave) : (a) P-5, (b) P-6, (c) P-7, and (d) P-8

6.2. Comparison of the observed peak values and the analytical results

The horizontal PGA observed at Fukiai (FKI) on the south side of R2 in the heavily damaged zone is 833 cm/s^2. The horizontal PGA in the principal direction observed at Kobe Harbor Office (KBH) in the reclaimed land is 538 cm/s^2. The corresponding PGV is 122 cm/s. These observation values are consistent with the analytical results, although the locations of these two points cannot be plotted in the analysed section because they are too far from the section. It is also noted that relatively large vertical motions are observed near the rock–sediment boundary. The vertical PGV observed at the third basement floor of the high-rise building near Shin Kobe station (SKB) is 47 cm/s compared to 31 and 25 cm/s for the two horizontal components.[2] The vertical PGV at Motoyama (KOB) is 49 cm/s compared to 55 and 77 cm/s for the two horizontal components, although these are the peak values of the restored velocity waveforms from the saturated records.[20] These observations seem consistent with the analytically estimated tendency for the vertical motions to be relatively large near the rock–sediment boundary (refer to Figure 10).

7. CONCLUDING REMARKS

In this study, wave propagation analyses were performed using the assumed 2D underground structure model normal to the Rokko geological faults based on the existing geological information. The incident wave is assumed to be a plane wave which is estimated by a deconvolution analysis using the observation record at Kobe University. Although there are qualifications due to the uncertain characteristics of the input rock motion and shear wave velocities of the underground structure, the following findings are obtained.

(1) It is shown analytically that the ground motion in the heavily damaged belt zone are amplified due to the focusing effect of the deep irregular underground structure as well as the shallow surface layers. It is

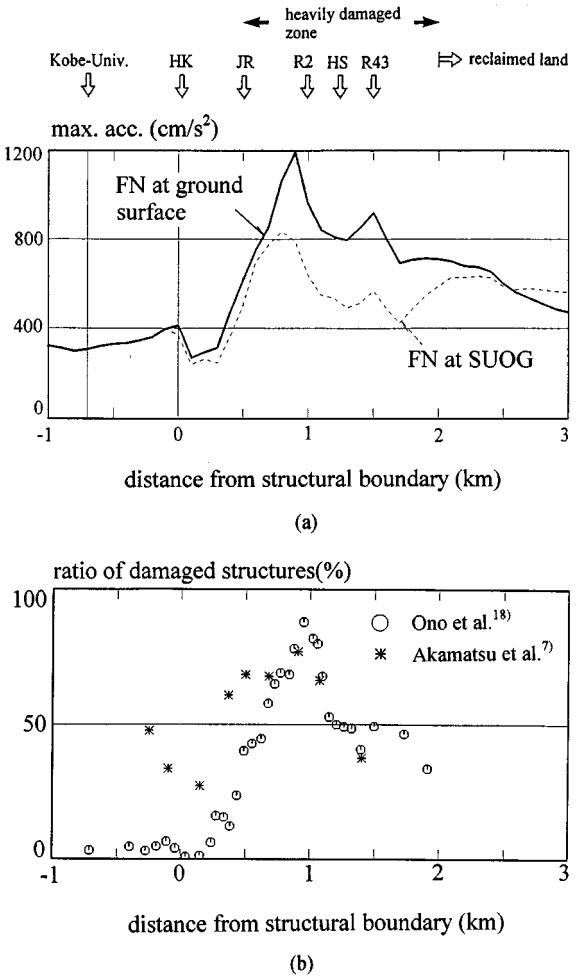

Figure 17. Comparison of the distributions of PGAs and structural damage. (a) Distributions of PGAs and (b) Structural damage ratios in Nada ward.[7,18] Damage surveys are performed near the analysed section along the a–a' line in Figure 1. The investigated structures are of wood and reinforced concrete (RC)

not necessary to incorporate the ground surface rupture of the seismic fault beneath the belt zone to explain the damaged zone.

(2) The calculated PGA distributions coincide closely with the structural damage distribution. It may thus be concluded that the explanation of the heavily damaged belt zone is the focusing effect in the deep irregular underground structure at the edge of the Osaka basin as well as the shallow surface layers. In future seismic design, it might be necessary to take into account the zoning factor due to irregular geological structures.

(3) It is suggested that the vertical motions were induced by the deep irregular underground structure, even if the incident wave field consists of only horizontal motion. The ratio of vertical motion to horizontal motion is less than half, with the exception of the sediment site in the vicinity of the vertical discontinuity, where a relatively large vertical motion was induced. It is necessary to investigate the effects of vertical motions on the structural response.

It is noted that structural damage is discussed not only from the intensity of ground motion, but also investigated from the viewpoint of seismic resistance capacity of structures.

The sensitivity of the results to the characteristics of the input rock motion and shear wave velocities of the subsurface materials including significant sources of uncertainty, should be further investigated to discuss quantitatively the results at next stage. The amplification characteristics of the ground motions in the analysed irregular structure should also be investigated for the complete incident wavefield, by considering a finite moving source with inhomogeneous slip distribution.

ACKNOWLEDGEMENTS

We are grateful to the Committee of Earthquake Observation and Research in Kansai Area (CEORKA), who provided valuable earthquake observation data and also valuable information on the velocity structure at the Kobe University site and the results along the Ishiyagawa measuring line obtained from the reflection survey referred to in this study. We also thank Dr. Takuji Kobori, Professor Emeritus of Kyoto University and Chief Advisor of Kajima Corporation, who provided valuable advice in this study.

REFERENCES

1. M. Takemura and Y. Tsuji, 'Strong motion distribution in Kobe area due to the 1995 Southern Hyogo Earthquake ($M = 7{\cdot}2$) in Japan as inferred from the topple rate of tombstones', *J. phys. earth* **43**, 747–753 (1995).
2. Building Research Institute (BRI), '*Interim Report* of damage survey during the 1995 Hyogo-ken Nanbu earthquake', 123–125 (1995) (in Japanese).
3. K. Toki, K. Irikura and T. Kagawa, 'Strong motion records in the source area of the Hyogoken-Nambu Earthquake, 17 January 1995, Japan', *J. natural disaster sci.* **16**, 23–30 (1995).
4. M. Watanabe and Y. Suzuki, 'Late Quaternary activity of active faults in Kobe area', *Programme and Abstracts*, The Seismological Society of Japan, **2**, A85 (1995) (in Japanese).
5. T. Suzuki, M. Hakuno and S. Igarashi, 'Numerical simulation on ground motion amplification on dipping soft soil layers', *Proc. 23rd JSCE earthquake engineering symp.*, 73–76 (1995) (in Japanese).
6. M. Motosaka and M. Nagano, 'Analysis on amplification characteristics of ground motions in Kobe City taking account of deep irregular underground structure — interpretation of heavily damaged belt zone during the 1995 Hyogo-ken Nanbu Earthquake', *J. struct. construction eng.* (*Trans. AIJ*), **488**, 39–48 (1996) (in Japanese with English abstract).
7. J. Akamatsu, H. Morikawa, H. Saito and M. Jido, 'Relation between the distribution of damage caused by the 1995 Hyogoken-Nambu earthquake and vibration characteristics inferred from microseisms', *J. natural disaster sci.* **16**, 63–70 (1995).
8. K. Nakagawa, 'Relation between earthquake ground failure and subsurface structure', *Proc. symp. on the Great Hanshin-Awaji earthquake and its geo-environments*, 233–238 (1995) (in Japanese).
9. Y. Iwasaki, 'Earthquake environment in Hanshin area and strong ground motions during the Hyogo-ken Nanbu earthquake', *Soil found.* **43**, 2–6 (1995) (in Japanese).
10. Y. Iwami, *Town and Soil in Kobe*, Kobe Shinbun Press Center, 1987, p. 14 (in Japanese).
11. S. Kobayashi, S. Yoshida, S. Okubo, R. Shichi, T. Shimamoto and T. Kato, '2·5-dimensional analysis of the gravity anomaly across the Rokko fault system', *Programme and Abstracts*, The Seismological Society of Japan, **2**, A61 (1995) (in Japanese).
12. Y. Iwasaki, T. Hongo, H. Yokota and S. Ito, 'Ground characteristics of the Rokko-dai (Kobe University) Ground Motion Monitoring Site', *Programme and Abstracts*, The Seismological Society of Japan, **2**, P77 (1995) (in Japanese).
13. T. Iwata, K. Hatayama, H. Kawase, K. Irikura and K. Matsunami, 'Aftershock observations at Higashinada ward, Kobe City', *J. natural disaster sci.* **16**, 41–48 (1995).
14. M. Nagano and M. Motosaka, 'Response analysis of 2-D structure subjected to obliquely incident waves with arbitrary horizontal angles', *J. struct. construction eng.* (*Trans. AIJ*) **474**, 67–76 (1995) (in Japanese with English abstract).
15. E. Kausel and J. M. Roesset, 'Semianalytical hyperelement for layered strata', *J. eng. mech. ASCE* **103**, 569–588 (1977).
16. Japan Society of Soil Mechanics and Foundation Engineering, Kansai branch, Soil in Kansai area, 1992 (in Japanese).
17. M. Imazu and K. Fukutake, 'Dynamic shear modulus and Damping of gravel materials', *Proc. 21st Japan national conf. on soil mechanics and foundation engineering*, 509–512 (1986) (in Japanese).
18. S. Ono, K. Ishikawa and S. Mizoguchi, 'Earthquake damage survey of buildings & houses during the 1995 Hyogo-ken Nanbu earthquake', *Proc. 50th ann. conf. of the Japan Society of Civil Engineers*, **1-(B)**, 948–949 (1995) (in Japanese).
19. Chuo Kaihatsu Corporation, *Report on damage survey of the 1995 Hyogo-ken Nanbu earthquake*, 1995 (in Japanese).
20. T. Kagawa, K. Irikura and I. Yokoi, 'Saturation characteristics of servo velocity seismograph—application for the records obtained under the Hyogoken-Nanbu earthquake', *Programme and Abstracts*, The Seismological Society of Japan, **2**, A91 (1995) (in Japanese).